First experimental test of X(5) critical-point symmetry in the $A \sim 130$ mass region: Low-spin states and the collective structure of ^{130}Ce

A. F. Mertz,[1,*] E. A. McCutchan,[1] R. F. Casten,[1] R. J. Casperson,[1] A. Heinz,[1] B. Huber,[1] R. Lüttke,[1,2] J. Qian,[1] B. Shoraka,[1,3] J. R. Terry,[1] V. Werner,[1] E. Williams,[1] and R. Winkler[1]

[1]*Wright Nuclear Structure Laboratory, Yale University, New Haven, Connecticut 06520, USA*

[2]*Technische Universität Darmstadt, D-64289 Darmstadt, Germany*

[3]*University of Surrey, Guildford, Surrey GU2 7XH, United Kingdom*

(Received 31 October 2007; published 10 January 2008)

Excited, low-spin states in ^{130}Ce are populated in the β^+/ϵ decay of ^{130}Pr and studied through off-beam γ-ray spectroscopy at the Yale moving tape collector. New coincidence data lead to the construction of a substantially revised level scheme. The low-lying states of ^{130}Ce are compared with the predictions of the X(5) critical-point model and the X(5)-β^4 model, and the latter is found to give better agreement with the data in terms of energies. Discrepancies in the relative $B(E2)$ values in ^{130}Ce and the geometrical models suggest that the γ degree of freedom may play an important role in this mass region.

DOI: 10.1103/PhysRevC.77.014307 PACS number(s): 21.10.Re, 21.60.Fw, 23.20.Lv, 27.60.+j

I. INTRODUCTION

One of the most important issues in current nuclear-structure studies is the evolution of structure as a function of the number of nucleonic constituents (N, Z). Atomic nuclei present a rich variety of structures, and twin themes are (1) to interpret the observed data in terms of geometric or algebraic models that account for the reasonably simple patterns observed and (2) to understand the origins of these patterns in terms of the underlying microscopic foundations in terms of nucleon motion and their interactions. This study addresses the first of these goals in an area of high current interest, namely, understanding the behavior of atomic nuclei in regions of substantial structural change, regions in which the concept of quantum phase transitions has recently proved extremely useful [1,2].

Following the development of a new set of benchmarks [1,2] describing the critical points of quantum phase transitions from spherical to quadrupole deformed shapes in atomic nuclei, a number of studies focused on the search for empirical examples. The critical-point symmetry denoted as X(5) [1] describes the behavior in a first-order quantum phase transition from a spherical harmonic vibrator to an axially deformed rotor with analytic solutions that are parameter-free except for scale. ^{152}Sm offered the first experimental evidence for X(5) [3], and subsequent studies on ^{150}Nd [4] and ^{154}Gd [5] also revealed good agreement with the X(5) model. In fact, the entire sequence of $N = 90$ nuclei from Ce to Dy demonstrates many features of X(5) [6], although some discrepancies do exist.

To date, most empirical searches for X(5) have concentrated on nuclei in the major shell region $Z = 50$–82 and $N = 82$–126, specifically near $N = 90$. Therefore, it is reasonable to wonder whether evidence for X(5) might exist in other areas of the nuclear chart. Since the interactions between valence protons and neutrons have a significant effect on collectivity and deformation [7], one quantity useful in identifying nuclei near the shape/phase transition is the P factor [8],

$$P = \frac{N_p N_n}{N_p + N_n}, \tag{1}$$

defined in terms of N_p and N_n, the numbers of valence protons and neutrons, respectively [9]. The numerator represents an approximate measure of the number of valence p-n interactions, and the denominator represents the strength of the pairing interaction (N_p+N_n) because each nucleon pairs with only one other in the time-reversed orbit. Since typical p-n interactions in heavy nuclei are $\sim$200 keV and the pairing interactions are $\sim$1 MeV, $P \sim 5$ is the point at which the p-n interaction begins to dominate. Thus, the locus of $P \sim 5$ on the N-Z plane provides a road map for finding nuclei potentially at the shape/phase transition described by X(5). Figure 1 shows the even-even nuclei with $P \sim 5$ in one section of the chart of the nuclides. Most previous experimental studies of X(5) have concerned nuclei in the right-hand part of the pictured locus where proton and neutrons fill different major shells. A nucleus in the left-hand part of the pictured locus would offer, for the first time, a comparison with X(5) in a region in which both valence protons and valence neutrons are in the same shell. Additionally, these nuclei, in which valence neutrons are considered "holes" according to the shell model, are symmetric across the $N = 82$ line to the previously studied nuclei, in which the valence neutrons are considered "particles." For that reason, an experiment on a nucleus in the left major shell region could test whether the underlying shell structure influences critical-point behavior, as well as offer insight into the breadth of nuclei that X(5) might describe. Furthermore, expanding the number of X(5) identified nuclei over a broader mass range could be useful in determining how the model's manifestations are N, Z dependent, which might have implications for exotic nuclei in new regions.

For this study, we selected the nucleus ^{130}Ce, with eight valence neutrons and ten valence protons, based on its P factor

*Present address: University of Oxford, Oxford OX1 4AR, United Kingdom.

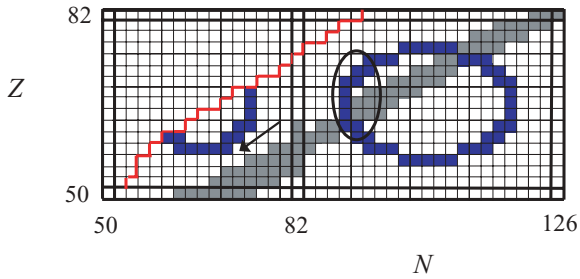

FIG. 1. (Color online) Portion of the nuclear chart showing the stable nuclei (grey boxes) and the locus of $P \sim 5$ where candidates for X(5) should appear [black (blue) boxes]. The oval indicates the region where X(5) experimental studies have been concentrated. The candidate nucleus for this study, ^{130}Ce, is indicated with an arrow. Figure adapted from Ref. [10].

of 4.4, which is not too far from the $P \sim 5$ prediction for X(5) candidates, and its $R_{4/2} \equiv E(4_1^+)/E(2_1^+)$ ratio of 2.80 [11], which is close to the value of 2.91 predicted by X(5) [1]. Further supporting our selection of ^{130}Ce for this study, an extensive empirical analysis of even-even nuclei with $Z \geqslant 20$, $N \geqslant 20$ identified ^{130}Ce as one of two nuclei outside the $N = 90$ isotones as the best potential X(5) candidates based on yrast energy states and yrast $B(E2; J \rightarrow J-2)$ values [12].

The purpose of this work is to identify the low-lying levels in ^{130}Ce, observe their depopulating transitions, and compare the findings to the X(5) critical-point model as well as other models which describe the low-lying, collective structure of nuclei.

II. EXPERIMENT

We populated low-lying states of ^{130}Ce through β^+/ϵ decay and analyzed the γ decay using off-beam γ-ray coincidence spectroscopy at the Yale moving tape collector [13]. The parent nuclei, ^{130}Pr, with $T_{1/2} = 40$ s, were produced through the ^{107}Ag(^{27}Al, $p3n$)^{130}Pr reaction by striking a 1.5-mg/cm^2 silver target with a ~5-pnA aluminum beam at 113 MeV generated by the Yale ESTU (extended stretched transuranium) tandem accelerator. The recoil product nuclei were implanted into a 16-mm-wide aluminized Kapton tape. To prevent the unreacted beam from reaching and subsequently vaporizing the tape, we placed a 3-mm-diameter gold plug 8.0 cm downstream of the target. Since the product nuclei were distributed in a geometrical cone, as in all fusion-evaporation reactions, the plug prevented the primary unreacted beam from reaching the tape while sacrificing only a small fraction of the product nuclei. The reacted nuclei with a wide-enough transmission angle, ~80% of the nuclei in this geometry, bypassed the plug and became imbedded in the tape. The tape advanced every 72 s, a rate that optimized the proportion of undecayed reacted nuclei reaching the shielded low-background counting area.

The detector array contained four Compton-suppressed segmented yrast ball clover HPGe detectors [14] in close geometry, with an array photopeak efficiency of 1.1% at 1.3 MeV and energy range from 40 keV to 2.4 MeV. Both γ-ray singles and γ-γ coincidence data were acquired in event

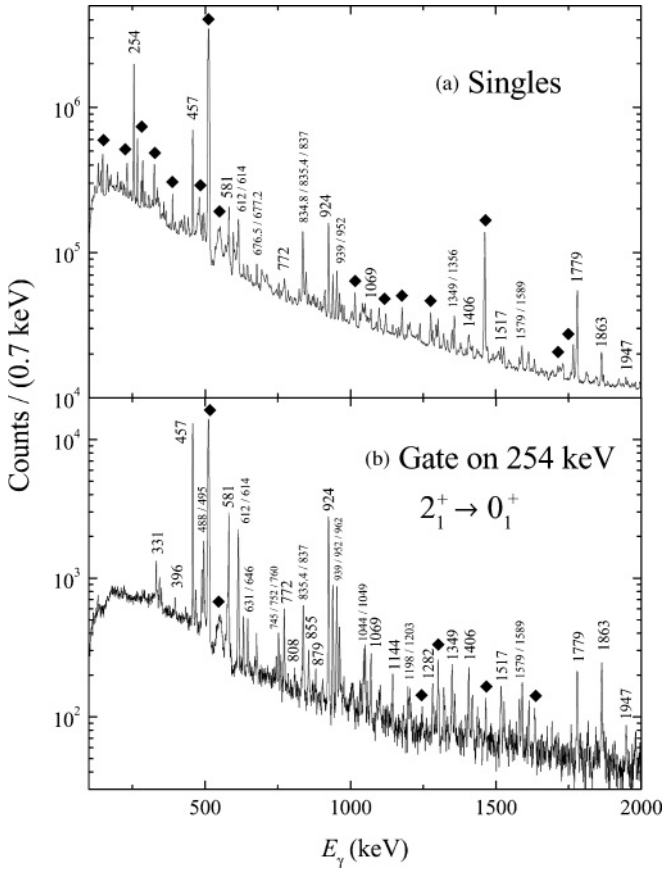

FIG. 2. (a) Clover-singles spectrum and (b) coincidence spectrum gated on the 254-keV, $2_1^+ \rightarrow 0_1^+$ transition. In both figures, the most intense transitions attributed to ^{130}Ce are labeled with their energy values, while contaminant and background lines are marked with a diamond (◆).

mode. The experiment lasted ~98 h and acquired 2.5 $\times 10^8$ clover singles and 2.0 $\times$ 10^7 clover-clover coincidence events. Figure 2(a) shows the summed clover singles spectrum, and Fig. 2(b) shows a sample γ-γ spectrum, gated on the 254-keV, $2_1^+ \rightarrow 0_1^+$ transition.

Table I reports the γ rays assigned to ^{130}Ce based on the γ-γ coincidences from the present experiment, including placements, intensities, and the most useful coincidence relations. Table II summarizes the levels populated in ^{130}Ce, including spin assignments where possible, along with a comparison of intensity values with those from the literature.

High-statistics coincidence data in the present study allowed the unique placement of transitions within the deduced level scheme and more reliable and precise measurements of γ-ray energies to confirm energy-sum relations. In this experiment, we found no support for two previously reported low-lying levels, found evidence for several new levels and transitions, and achieved enough statistics to make more precise determinations of the relative intensities of transitions. In completing this work, we consulted the evaluated data [11], as well as a more recent study by Gizon *et al.* [15] in which a number of new levels and transitions were observed. In the following discussion, the intensities given are normalized to the intensity of the 254-keV, $2_1^+ \rightarrow 0_1^+$ transition ($I_{254} \equiv$

TABLE I. Observed γ-ray transitions in ^{130}Ce, arranged in order of increasing transition energy. Relative (in β decay) intensities [normalized to $I_{254} \equiv 100$] and the most useful coincidence relations are given.

E_γ (keV)	E_i (keV)	E_f (keV)	I_γ	Coincidences[a]
253.91(3)	253.91	0.00	100(3)	457, 488, 495, 577, 581, 924, 938, 952
330.87(5)[b]	1356.5	1025.5	1.4(1)	254, 498, 676.5, 772, 760
342.83(5)	1177.61	834.81	2.1(1)	254, 495, 581, 834.8, 938, 952
349.1(1)[c]	1672.3	1323.15	0.97(12)	254, 457, 488, 581, 952
396.0(3)[d]	2068.1	1672.3	0.79(9)	254, 457, 495, 581, 784, 924, 962
456.66(3)	710.58	253.91	47.3(14)	254, 467, 631, 646, 952, 962, 1044, 1049
467.00(5)	1177.61	710.58	1.6(1)	254, 457, 495, 938, 952
470.6(4)[d]	2624.3	2154.0	0.51(8)	254, 581, 834.8, 924, 976, 1319
477.1(4)[d]	1833.4	1356.5	0.32(6)	1035, 1356
488.3(1)	1323.15	834.81	4.7(2)	254, 349, 574, 581, 834.8, 1204
494.5(2)	1672.3	1177.61	5.3(3)	254, 343, 457, 467, 834.8, 879, 952, 1032
498.04(4)[b]	1854.6	1356.5	0.97(10)	254, 331, 457, 646, 772, 1356
572.8(4)[e]	1897.6	1324.69	0.57(5)	614
574.5(2)[e]	1897.6	1323.15	0.34(4)	254, 457, 488, 581, 613, 834.8
577.2(1)	1754.8	1177.61	2.1(1)	254, 343, 457, 924
580.91(5)	834.81	253.91	12.2(6)	254, 349, 471, 488, 837, 952, 1319, 1869
588.0(4)[c]	2704.3	2116.2	0.39(8)	254, 760, 924, 938, 1282, 1406, 1862
612.6(4)	1323.15	710.58	4.9(4)	254, 457, 349, 574, 745, 1101, 1203
614.11(4)	1324.69	710.58	6.9(3)	254, 457, 784, 1058, 1527
631.2(2)	1955.9	1324.69	1.5(1)	254, 457, 614
645.7(1)[d]	1356.5	710.58	1.0(1)	254, 457, 498, 676.5, 760
672(1)[d]	2704.3	2032.9	0.61(13)	254, 1779
676.5(2)[d]	2032.9	1356.5	1.1(1)	254, 331, 457, 646, 772, 924
677.2(5)[d]	1854.6	1177.61	0.23(6)	254, 331, 457, 646, 772, 834.8, 924
743.6(3)[d,e]	2068.1	1324.69	0.16(9)	614
744.7(4)[d,e]	2068.1	1323.15	0.69(14)	254, 457, 488, 581, 784, 1069
752.2(4)[d]	2868.4	2116.2	1.1(2)	254, 457, 760, 924, 938, 1406, 1862
759.8(3)[d]	2116.2	1356.5	0.79(9)	254, 331, 646, 752, 1356
771.64(8)	1025.5	253.91	2.4(1)	254, 331, 498, 677.2, 760, 808, 1035
784.4(9)[d]	2852.2	2068.1	0.43(9)	254, 396, 457, 745, 834.8, 837, 1358
793.1(7)[b]	3020.8	2226.8	0.08(3)	254, 457, 1516
807.6(1)[d]	1833.4	1025.5	0.44(4)	254, 772, 1035
834.80(7)	834.81	0.00	9.1(3)	343, 488, 495, 952, 1319, 1869
835.4(4)[d]	2868.4	2032.9	2.3(2)	676.5, 855, 1779
837.3(1)	1672.3	834.81	4.6(2)	254, 396, 581, 879, 952, 1032, 1198
855.2(2)[d]	2032.9	1177.61	0.77(8)	254, 924, 835.4
879.4(3)[f]	2551.5	1672.3	0.64(15)	254, 494, 581, 835.8, 837, 924, 1418
903.4(3)[d]	2226.8	1323.15	0.39(8)	254, 457, 488, 581, 834.8, 1069
923.66(8)	1177.61	253.91	18.1(5)	254, 396, 495, 752, 879, 952, 976
938.5(2)	2116.2	1177.61	5.3(2)	254, 343, 457, 467, 581, 752, 924
952.3(1)	2624.3	1672.3	6.2(3)	254, 343, 349, 457, 581, 834.8, 924, 962
961.61(6)	1672.3	710.58	2.1(1)	254, 457, 952, 1032
976.0(2)[b]	2154.0	1177.61	0.41(8)	254, 471, 924
1002(1)[d]	2868.4	1866.7	0.19(4)	1613
1004.0(5)[f]	2760	1754.8	0.38(9)	254, 457, 577, 924, 1044
1032.0(4)[d]	2704.3	1672.3	0.78(13)	254, 457, 495, 581, 834.8, 837, 924, 962
1035.4(1)[d]	2868.4	1833.4	0.54(10)	254, 772, 808, 1579, 1833
1044.2(2)	1754.8	710.58	1.4(1)	254, 457, 1004
1049.34(3)[b]	1759.9	710.58	1.5(1)	254, 457
1057.5(2)	2382.2	1324.69	0.36(4)	254, 457, 614
1069.4(1)	1323.15	253.91	1.5(1)	254, 745, 903
1101(1)[f]	2423	1323.15	0.30(6)	254, 457, 488, 581, 613, 834.8
1102.8(5)[d]	1356.5	253.91	0.47(9)	254, 760
1144.3(9)[d]	1854.6	710.58	1.0(1)	254, 457
1197.7(7)[d]	2868.4	1672.3	0.31(7)	254, 495, 581, 834.8, 837, 924
1203.0(5)[d]	2526.1	1323.15	0.61(10)	254, 488, 581, 613, 834.8

TABLE I. (*Continued*.)

E_γ (keV)	E_i (keV)	E_f	I_γ	Coincidences[a]
1281.6(4)	2116.2	834.81	1.2(1)	254, 581, 752, 834.8
1300.4(2)[d]	2011.4	710.58	0.38(8)	254, 457
1319.4(5)[d]	2154.0	834.81	1.3(1)	254, 457, 471, 581, 834.8
1322.7(4)[c]	2032.9	710.58	0.47(7)	254, 457, 835.4
1348.7(2)[c]	2059.3	710.58	1.5(1)	254, 457
1356.44(5)[d]	1356.5	0.00	3.4(2)	498, 676.5, 760
1357.73(5)[d]	2068.1	710.58	0.72(8)	254, 457, 784
1405.7(1)	2116.2	710.58	1.5(1)	254, 457, 752
1418.4(1)[d]	1672.3	253.91	0.60(8)	254, 952
1435.6(3)[f]	2760.	1324.69	0.18(5)	254, 457, 614
1516.5(2)[d]	2226.8	710.58	1.3(1)	254, 457, 793
1527.5(9)[d]	2852.2	1324.69	0.31(6)	254, 457, 614
1579.3(2)[d]	1833.4	253.91	0.70(9)	254, 1035
1589.08(6)[c]	2299.7	710.58	1.4(1)	254, 457
1612.7(4)[d]	1866.7	253.91	0.75(9)	254, 1002
1757.8(4)[d]	2011.4	253.91	1.4(1)	254
1779.14(10)[d]	2032.9	253.91	2.1(1)	254, 835.4
1815.4(3)[d]	2526.1	710.58	0.33(6)	254, 457
1833(1)[d]	1833.4	0.00	0.28(9)	1035
1862.2(5)[c]	2116.2	253.91	2.5(1)	254, 752
1869(1)[d]	2704.3	834.81	0.76(12)	254, 581, 834.8
1946.9(4)[c]	2657.5	710.58	0.78(10)	254, 457
2033(1)[d,f]	2032.9	0.00	0.33(3)	
2310.7(5)[d]	3020.8	710.58	0.66(8)	254, 457

[a]Only those coincident transitions most relevant to the placement of the tabulated transition or to measurement of its intensity are listed. For low-lying transitions coincident with a large number of feeding transitions, weaker feeding transitions are omitted.
[b]γ-ray line was reported in Ref. [15] in alternative location.
[c]γ-ray line was observed in Ref. [15] but not in Ref. [11].
[d]γ-ray line was not previously reported [11,15].
[e]Transitions from the closely spaced levels at 1323.15 and 1324.69 keV are most likely doublets. Each transition is assigned a primary placement as depopulating one of these levels on the basis of the transition energy measured in a gated spectra but may contain an unresolved contribution from the other depopulating member of the pair. The large relative error in the intensities is due to the inability to resolve the two close energies in gated spectra.
[f]Placement of transition is tentative.

100), and relative intensities are normalized to the strongest branch from each level ($I^{\rm rel} \equiv 100$). We took spin assignments from Ref. [11,15] unless we obtained information from the present experiment affecting the previous spin assignments. Figure 3 shows the level scheme we deduced from the present experiment for level energies below 2.1 MeV.

2_2^+ *at 835 keV.* The intensity values for the two depopulating transitions from the first excited 2^+ state determined in the present experiment agree with values from Ref. [11] but not with those from Ref. [15]. A gate on the 488-keV transition, which directly feeds the level at 835 keV, yielded a spectrum with the ratio of the area of the 581-keV line to the area of the 834.8-keV line to be approximately 7:4. These areas, with appropriate efficiency corrections taken into consideration, clearly showed that the intensity of the 581-keV transition is greater than that of the 834.8-keV transition, confirming the values reported by Ref. [11].

(2^+) *at 1305 keV.* Reference [15] identified an excited (2^+) state with energy 1305 keV, 280 keV above the first excited 0^+ state at 1025 keV (1026 keV according to our energy calibration), based on three depopulating transitions with energies 280, 596, and 1051 keV, decaying to the 0_2^+, 4_1^+, and 2_1^+ states, respectively. However, in the present experiment, a gate on the 1051-keV peak (1049 keV according to our energy calibration) produced strong coincidences with both the 254- and 457-keV transitions (Fig. 4). Therefore we provide an alternative placement for the 1049-keV transition as directly populating the 4_1^+ state. A gate on the 280-keV line yielded strong coincidences only with 308- and 774-keV transitions in ^{131}Ce [16], produced in a competing reaction channel. No support was found for the previously identified 596-keV transition, as a gate on this energy yielded no coincidences with any identified transitions in ^{130}Ce. With no evidence for any of the previously reported depopulating transitions, we eliminated the level at 1305 keV. This revision has important consequences for the discussion of structure below.

4_2^+ *at 1323 keV.* References [11,15] report an excited 4^+ state at 1323 keV, and the present experiment shows

TABLE II. Levels populated in ^{130}Ce and their γ decay. Intensities are given for γ-ray transitions depopulating the levels and compared with literature values [11,15] where available. Intensity limits are given for spin-allowed but unobserved transitions between low-lying levels relevant to the structural interpretation of the nucleus. For these limits, the approximate transition energy expected from the level energy difference is shown in brackets. For levels above 2 MeV, the tentative spin assignments are based on observed transitions to levels of known spin.

J_i^π	E_i (keV)	J_f^π	E_f (keV)	E_γ (keV)	I_γ	I_γ^{rel}	$I_{\gamma\mathrm{lit}}^{\mathrm{rel}}$[a]	$I_{\gamma\mathrm{lit}}^{\mathrm{rel}}$[b]
2^+	253.91(3)	0^+	0.00	253.91(3)	100(3)	100(3)	100	100
4^+	710.58(4)	2^+	253.91	456.66(3)	47.3(14)	100(3)	100	100(7)
2^+	834.81(5)	4^+	710.58	[124]	<0.04			
		2^+	253.91	580.91(5)	12.2(6)	100(5)	100(10)	88(4)
		0^+	0.00	834.80(7)	9.1(3)	74(2)	80(9)	100(6)
0^+	1025.5(1)	2^+	834.81	[191]	<0.04			
		2^+	253.91	771.64(8)	2.4(1)	100(4)		100(14)
3^+	1177.61(5)	2^+	834.81	342.83(5)	2.1(1)	11(1)	7(2)	5(2)
		4^+	710.58	467.00(5)	1.6(1)	8.9(5)	9(3)	13(1)
		2^+	253.91	923.66(8)	18.1(5)	100(3)	100(7)	100(5)
4^+	1323.15(5)	3^+	1177.61	[146]	<0.04			
		2^+	834.81	488.3(1)	4.7(2)	97(4)	69(21)	100(6)
		4^+	710.58	612.6(4)	4.9(4)	100(9)	100(23)	6(3)
		2^+	253.91	1069.4(1)	1.5(1)	31(2)	22(6)	17(3)
6^+	1324.69(6)	4^+	710.58	614.11(4)	6.9(3)	100(4)	100	100(8)
2^+	1356.5(2)[c]	3^+	1177.61	[179]	<0.19			
		0^+	1025.5	330.87(5)[d]	1.4(1)	41(2)		
		2^+	834.81	[521]	<0.03			
		4^+	710.58	645.7(1)[e]	1.0(1)	31(3)		
		2^+	253.91	1102.8(5)[e]	0.47(9)	14(3)		
		0^+	0.00	1356.44(5)[e]	3.4(2)	100(6)		
$(2^+, 3, 4^+)$	1672.3(2)	2^+	1356.5	[316]	<0.06			
		4^+	1323.15	349.1(1)[f]	0.97(12)	11(1)		11(5)
		3^+	1177.61	494.5(2)	5.3(3)	100(5)	26(8)	100(5)
		2^+	834.81	837.3(1)	4.6(2)	85(4)	100(5)	80(7)
		4^+	710.58	961.61(6)	2.1(1)	40(2)	22(9)	36(7)
		2^+	253.91	1418.4(1)[e]	0.60(8)	11(1)		
(5^+)	1754.8(2)	4^+	1323.15	[432]	<0.19			
		3^+	1177.61	577.2(1)	2.1(1)	100(5)	100	100(33)
		4^+	710.58	1044.2(2)	1.4(1)	68(5)		60(20)
	1759.9(1)[g]	4^+	710.58	1049.34(3)[d]	1.5(1)	100(7)		
$(1, 2^+)$	1833.4(6)[c]		1672.3	[161]	<0.04			
		2^+	1356.5	477.1(4)[e]	0.32(6)	45(9)		
		0^+	1025.5	807.6(1)[e]	0.44(4)	62(6)		
		2^+	834.81	[999]	<0.12			
		2^+	253.91	1579.3(2)[e]	0.70(9)	100(12)		
		0^+	0.00	1833(1)[e]	0.28(9)	41(13)		
$(2^+, 3, 4^+)$	1854.6(2)[c]	(5^+)	1754.8	[100]	<0.02			
			1672.3	[182]	<0.04			
		2^+	1356.5	498.04(4)[d]	0.97(10)	98(10)		
		6^+	1324.69	[530]	<0.05			
		4^+	1323.15	[531]	<0.03			
		3^+	1177.61	677.2(5)[e]	0.23(6)	23(6)		
		2^+	834.81	[1020]	<0.03			
		4^+	710.58	1144.3(9)[e]	1.0(1)	100(9)		
		2^+	253.91	[1601]	<0.04			
	1866.7(5)[g]	2^+	253.91	1612.7(4)[e]	0.75(9)	100(12)		
(6^+)	1897.6(3)		1759.9	[138]	<0.01			
		(5^+)	1754.8	[143]	<0.08			

TABLE II. (*Continued*.)

J_i^π	E_i (keV)	J_f^π	E_f (keV)	E_γ (keV)	I_γ	I_γ^{rel}	$I_{\gamma\mathrm{lit}}^{\mathrm{rel}}$ [a]	$I_{\gamma\mathrm{lit}}^{\mathrm{rel}}$ [b]
			1672.3	[225]	<0.04			
		2^+	1356.5	[541]	<0.12			
		6^+	1324.69	572.8(4)[h]	0.57(5)	100(9)	100(20)	71(29)
		4^+	1323.15	574.5(2)[h]	0.34(4)	56(6)	83(17)	100(43)
		3^+	1177.61	[720]	<0.03			
		2^+	834.81	[1063]	<0.18			
		4^+	710.58	[1187]	<0.03			
		2^+	253.91	[1644]	<0.04			
(5^-)	1955.9(3)	6^+	1324.69	631.2(2)	1.5(1)	100(7)		
$(2^+, 3, 4^+)$	2011.4(7)[c]	4^+	710.58	1300.4(2)[e]	0.38(8)	27(6)		
		2^+	253.91	1757.8(4)[e]	1.4(1)	100(5)		
(2^+)	2032.9(3)[j]	2^+	1356.5	676.5(2)[e]	1.1(1)	54(6)		
		3^+	1177.61	855.2(2)[e]	0.77(8)	36(4)		
		4^+	710.58	1322.7(4)[f]	0.47(7)	22(3)		43(14)
		2^+	253.91	1779.14(10)[e]	2.1(1)	100(6)		100(14)
		0^+	0.00	2033(1)[e,i]	0.33(3)	15(1)		
	2059.3(4)[j]	4^+	710.58	1348.7(2)[f]	1.5(1)	100(7)		100(20)
$(4^+, 5, 6^+)$	2068.1(3)[c]		1672.3	396.0(3)[e]	0.79(9)	100(11)		
		6^+	1324.69	743.6(3)[e,h]	0.16(9)	20(11)		
		4^+	1323.15	744.7(4)[e,h]	0.69(14)	87(18)		
		4^+	710.58	1357.73(5)[e]	0.72(8)	92(10)		
$(2^+, 3, 4^+)$	2116.2(2)	2^+	1356.5	759.8(3)[e]	0.79(9)	15(2)		
		3^+	1177.61	938.5(2)	5.3(2)	100(4)	100(21)	100(5)
		2^+	834.81	1281.6(4)	1.2(1)	23(3)		43(10)
		4^+	710.58	1405.7(1)	1.5(1)	29(2)	85(26)	13(8)
		2^+	253.91	1862.2(5)[f]	2.5(1)	47(3)		98(13)
	2154.0(5)[c]	3^+	1177.61	976.0(2)[d]	0.41(8)	31(6)		
		2^+	834.81	1319.4(5)[e]	1.3(1)	100(11)		
	2226.8(4)[c]	4^+	1323.15	903.4(3)[e]	0.39(8)	29(6)		
		4^+	710.58	1516.5(2)[e]	1.3(1)	100(8)		
	2299.7(2)[j]	4^+	710.58	1589.08(6)[f]	1.4(1)	100(7)		
	2382.2(3)	6^+	1324.69	1057.5(2)	0.36(4)	100(10)		
	2423(1)[g]	4^+	1323.15	1101(1)[i]	0.30(6)	100(21)		
	2526.1(3)[c]	4^+	1323.15	1203.0(5)[e]	0.61(10)	100(16)		
		4^+	710.58	1815.4(3)[e]	0.33(6)	53(10)		
	2551.5(5)[g]		1672.3	879.4(3)[i]	0.64(15)	100(23)		
	2624.3(8)		2154.0	470.6(4)[e]	0.51(8)	8.1(12)		
			1672.3	952.3(1)	6.2(3)	100(4)		100(6)
	2657.5(5)[j]	4^+	710.58	1946.9(4)[f]	0.78(10)	100(12)		100(23)
	2704.3(5)[j]		2116.2	588.0(4)[f]	0.39(8)	50(10)		
		(2^+)	2032.9	672(1)[e]	0.61(13)	79(17)		
			1672.3	1032.0(4)[e]	0.78(13)	100(17)		
		2^+	834.81	1869(1)[e]	0.76(12)	98(16)		
	2760(1)[k]	(5^+)	1754.8	1004.0(5)[i]	0.38(9)	100(25)		
		6^+	1324.69	1435.6(3)[i]	0.18(5)	48(12)		
	2852.2(8)[c]		2068.1	784.4(9)[e]	0.43(9)	100(20)		
		6^+	1324.69	1527.5(9)[e]	0.31(6)	71(13)		
	2868.4(6)[c]		2116.2	752.2(2)[e]	1.1(2)	46(7)		
		(2^+)	2032.9	835.4(4)[e]	2.3(2)	100(10)		
			1866.7	1002(1)[e]	0.19(4)	8.0(16)		
			1833.4	1035.4(1)[e]	0.54(10)	23(4)		
			1672.3	1197.7(7)[e]	0.31(7)	13(3)		

TABLE II. (*Continued.*)

J_i^π	E_i (keV)	J_f^π	E_f (keV)	E_γ (keV)	I_γ	I_γ^{rel}	$I_{\gamma\text{lit}}^{\text{rel}}$ [a]	$I_{\gamma\text{lit}}^{\text{rel}}$ [b]
	3020.8(8)[c]		2226.8	793.1(7)[d]	0.08(3)	13(54)		
		4^+	710.58	2310.7(5)[e]	0.66(8)	100(12)		

[a]Literature values for relative intensities are from Ref. [11].
[b]Literature values for relative intensities are from Ref. [15]. These values are provided because Ref. [11] did not include them at the time of publication.
[c]Level was not previously reported in β decay [11,15].
[d]γ-ray line was reported in Ref. [15] in alternative location.
[e]γ-ray line was not previously reported [11,15].
[f]γ-ray line was observed in Ref. [15] but not in Ref. [11].
[g]Level is tentatively assigned due to only a single observed depopulating transition.
[h]Transitions from the closely spaced levels at 1323.15 and 1324.69 keV are most likely doublets. Each transition is assigned a primary placement as depopulating one of these levels on the basis of the transition energy measured in a gated spectra but may contain an unresolved contribution from the other depopulating member of the pair. The large relative error in the intensities is due to the inability to resolve the two close energies in gated spectra.
[i]Placement of transition is tentative.
[j]Level was observed in Ref. [15] but not in Ref. [11].
[k]Level is tentatively assigned due to two low-intensity depopulating transitions.

three depopulating transitions with energies 488, 613, and 1069 keV that confirm this level. However, Refs. [11,15] reported conflicting values for the relative intensities of these transitions, with Ref. [15] identifying the strongest branch to be the 488-keV line and the 612-keV line with a relative intensity of 6(3). As Fig. 5 shows, a gate in the present experiment on the 349 keV populating transition generated a spectrum with the 488- and 613-keV lines having approximately equal areas. These areas, when corrected for efficiency, yielded relative intensity values of 100(9) and 97(4), respectively, in closer

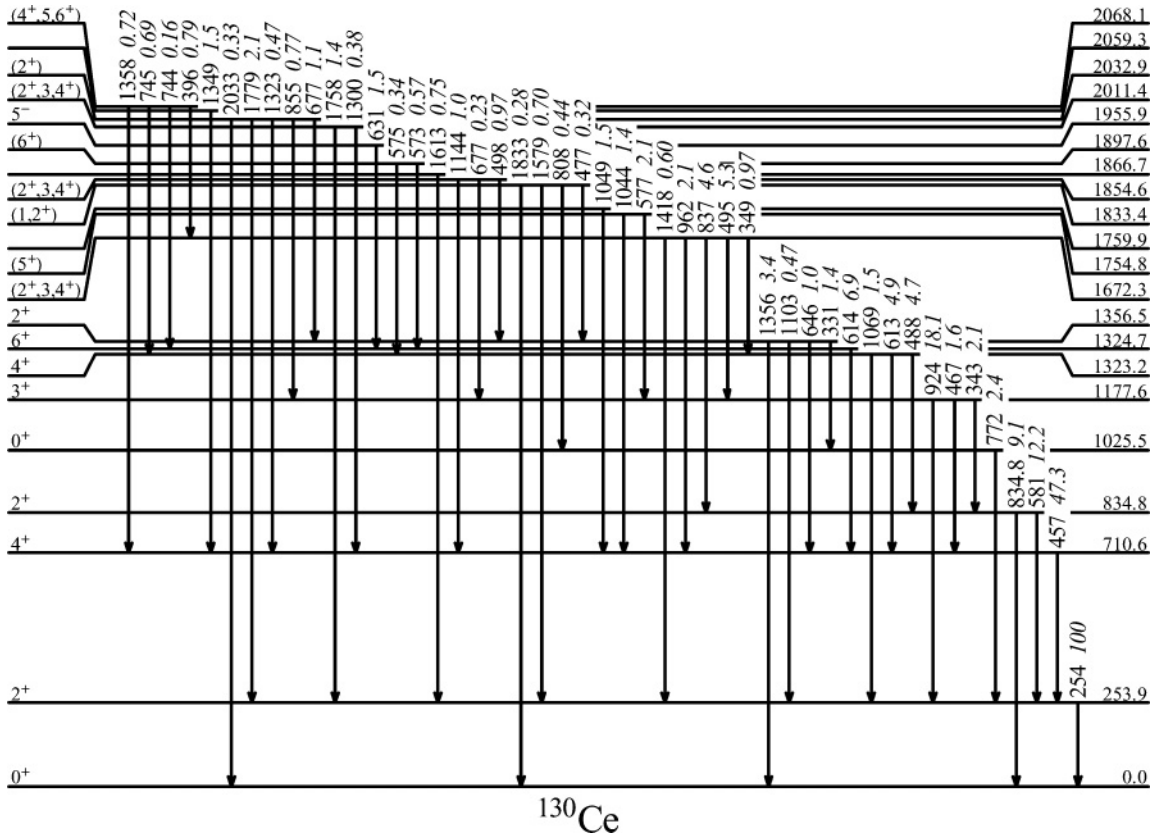

FIG. 3. Partial level scheme for ^{130}Ce deduced in this work. Level and transition energies are given in keV and intensities written in italics are normalized to the 254-keV, $2_1^+ \rightarrow 0_1^+$ transition ($I_{254} \equiv 100$).

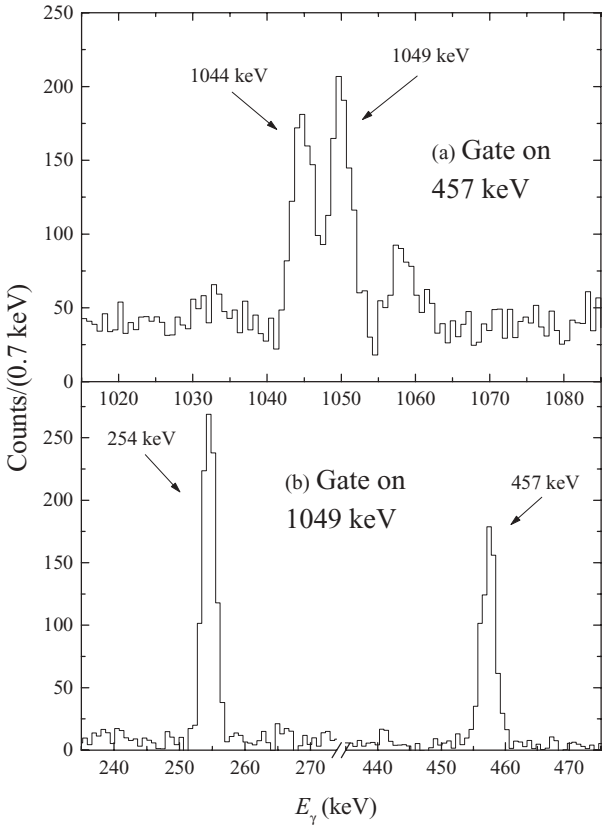

FIG. 4. Gated coincidence spectra giving evidence for the elimination of the previously identified (2^+) level at 1305 keV. The two spectra show that 1049 keV and 457 keV are in coincidence with each other, proving that the 1049-keV transition cannot feed directly into the 2_1^+ at 254 keV.

agreement with the values reported by Ref. [11] than those reported by Ref. [15].

2^+ *at 1357 keV.* We identify a new level at 1357 keV based on four previously unidentified depopulating transitions. We found a 331-keV transition with intensity 1.4(1) to be in strong coincidence with the 772-keV, $0_2^+ \rightarrow 2_1^+$ transition [Fig. 6(a)]. We also found a 646-keV transition with intensity 1.0(1) to be in coincidence with the 457-keV, $4_1^+ \rightarrow 2_1^+$ transition [Fig. 6(b)]. A spectrum comprised of the sum of the gates on the 676.5- and 760-keV peaks which feed into the level at 1357 keV [Fig. 6(c)] returned these 331- and 646-keV transitions, in addition to providing evidence for a 1103-keV line that decays to the 2^+ of the ground-state band. This summed gate also provides support for a transition from the 1357-keV line to the ground-state 0^+. This level is further supported by a number of populating transitions (Table I). Since the level at 1357 keV deexcites to levels with spin 0^+, 2^+, and 4^+, the most likely spin assignment for the 1357-keV level is 2^+.

Level at 1833 keV. We identified a new level at 1833 keV based on four depopulating transitions of energies 477, 808, 1579, and 1833 keV. These transitions were in strong coincidence with multiple depopulating transitions (except the 1833-keV line, which decays to the ground state) and feeding transitions, as reported in Table I. Because this level has transitions to states with spin 2^+ and 0^+, we narrowed the spin assignment of the 1833-keV level to $(1, 2^+)$.

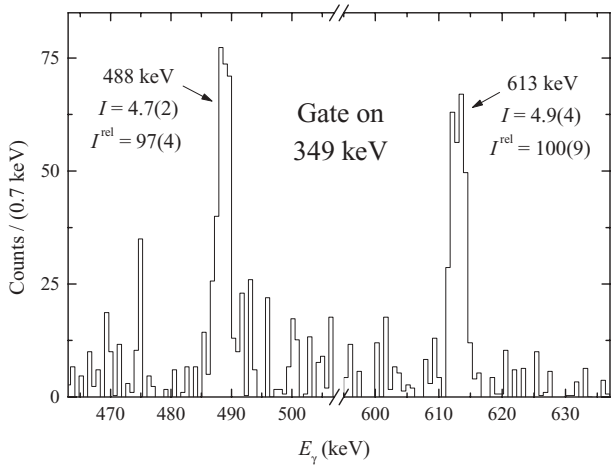

FIG. 5. Spectrum gated on feeding transition with 349 keV showing that the areas, and therefore the intensities, of the 488- and 613-keV transitions are approximately equal.

Level at 1855 keV. We identified a new level at 1855 keV based on three depopulating transitions of energies 498, 677.2, and 1144 keV, which decay to 2_2^+, 3_1^+, and 4_1^+ levels, respectively. Evidence for the 498-keV transition came from the observed coincidence with the 331-keV transition [Fig. 6(a)], as well as coincidences with other deexcitation transitions provided in Table I. We placed the transition with energy 677.2 keV based on a coincidence with the 924-keV, $3_1^+ \rightarrow 2_1^+$ transition. We determined the transition with energy 1144 keV feeds into the 4_1^+ level because of evidence for coincidences only with the 457-keV, $4_1^+ \rightarrow 2_1^+$ transition [Fig. 6(b)] and the depopulating transition with energy 254 keV. Since we could only identify transitions from this level to states with spin 2^+, 3^+, and 4^+, we could restrict the spin of the 1855 keV level only to $(2^+, 3, 4^+)$.

Remaining levels. Below 2 MeV, we also tentatively placed two levels (1760 and 1956 keV) based on only one depopulating transition. Above 2 MeV, we identified eight new levels that have multiple depopulating transitions with relatively strong intensities. Additionally, we tentatively placed three levels (2423, 2552, and 2760 keV) based on only one or two depopulating transitions. Since these levels were not essential in our analysis of the collective structure of ^{130}Ce, we forego detailed discussion on them.

III. DISCUSSION

^{130}Ce was proposed as a good candidate for X(5) structure in Ref. [12] based on yrast energies and $B(E2; J \rightarrow J-2)$ values. The X(5) solution is derived in the framework of the Bohr Hamiltonian by taking an infinite square well in the β deformation and a harmonic oscillator in the γ degree of freedom. The resulting predictions for energies and $E2$ transition strengths are parameter free except for scale. With new information on non-yrast structures, we first perform a detailed comparison of ^{130}Ce with the X(5) predictions.

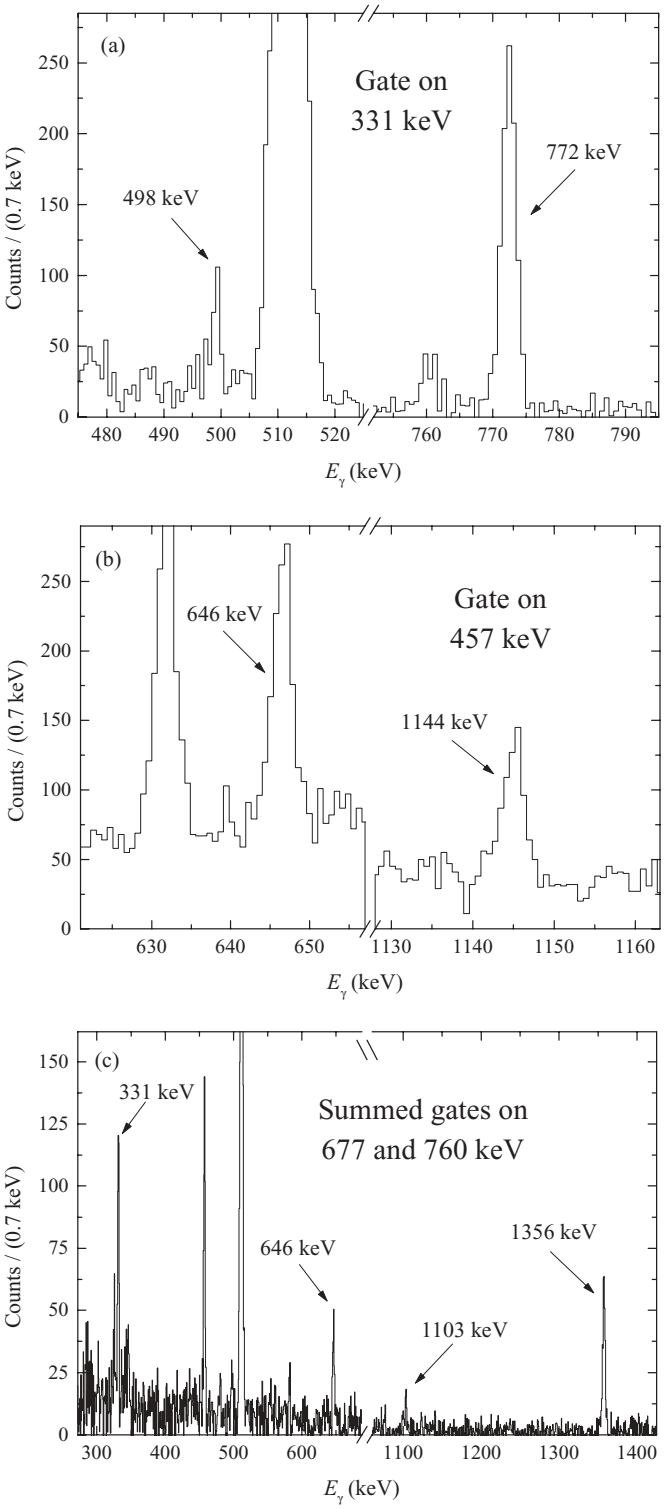

FIG. 6. Spectra providing evidence for a newly identified level at 1357 keV. (a) Spectrum gated on the 331 keV transition. (b) Spectrum gated on the 457 keV transition. (c) Summed spectra gated on 676.5- and 760-keV transitions. The 457-keV peak is relatively strong because the gate on 676.5 keV also includes much of the peak at 677.2 keV, which is in strong coincidence with the 457-keV, $4_1^+ \rightarrow 2_1^+$ transition.

The energy spacing within the yrast band of ^{130}Ce is reasonably reproduced by the X(5) predictions, as shown in Fig. 7. The $R_{4/2}$ ratio of 2.80 in ^{130}Ce is slightly less than the X(5) prediction of 2.90. Another important signature of X(5) is the prediction of the energy for the first excited 0^+ state at 5.67 times that of the energy of the 2_1^+ state. As shown in Fig. 7, the energy of the first excited 0^+ state is lower in ^{130}Ce, with $E(0_2^+)/E(2_1^+) = 4.0$.

In the present work, we find no evidence for the previously proposed 2^+ member of the 0_2^+-band sequence at 1305 keV. The newly observed 2^+ level at 1357 keV is the most likely candidate for the 2^+ member of the 0_2^+-band sequence. Below 1600 keV, it is the only level not assigned to a particular band structure. This gives an experimental 2^+-0^+ spacing in the excited band of 331 keV, somewhat less than the X(5) prediction of 460 keV. Larger than observed yrare energies are also typical of X(5) in the $N = 90$ region and have been associated with the steepness of the outer potential wall [17].

We tentatively assign the level at 1855 keV to be the 4^+ member of the 0_2^+-band sequence. This assignment is based on the fact that the 1855-keV level decays to the 2^+ level at 1357 keV, suggesting a possible band structure. With this assignment, the $R_{4/2}$ ratio in the excited 0^+ band is 2.50, again less than the X(5) predictions of 2.70. Still, the structure of ^{130}Ce is more or less consistent with the X(5) predictions, namely, an excited 0^+ band which is less deformed than the ground-state band.

Included in Fig. 7 are the relative $B(E2)$ transition strengths normalized to the intraband transition. Relative to the intraband transition, the interband $B(E2)$ strengths are significantly weaker in ^{130}Ce compared with the X(5) predictions for both the 2^+ and 4^+ members of the 0_2^+-band sequence. In the case of the 2^+ decay, all interband transition strengths are weaker by at least an order of magnitude in ^{130}Ce compared with the X(5) predictions. Again, this resembles (but is more extreme than) the situation in Sm and Nd with $N = 90$.

From the standpoint of the $R_{4/2}$ and the $E(0_2^+)/E(2_1^+)$ ratios, ^{130}Ce appears to lie slightly to the vibrational side of the critical point. Inspired by the X(5) solution, new geometrical models are being developed to describe a wider range of structures from spherical to axially symmetric deformed. Appropriate for ^{130}Ce is the X(5)-β^n model [18] which replaces the infinite square well potential with potentials of the form $u(\beta) = \beta^{2n}$, with n being an integer. With increasing powers of n, this model allows one to describe structures ranging from vibrational to X(5) as n goes to infinity. The predictions of the X(5)-β^n model are also parameter-free except for scale. Starting from the $R_{4/2}$ and the $E(0_2^+)/E(2_1^+)$ ratios, we found that X(5)-β^4 gives the best agreement with the data on ^{130}Ce among all the X(5)-β^n models. A comparison between the X(5)-β^4 predictions and ^{130}Ce is included in Fig. 7. The X(5)-β^4 model almost exactly reproduces both the yrast band energies as well as the 0_2^+-band energies. For the 0_2^+ sequence, both the bandhead energy, as well as the spacings within the band, are very well described by the X(5)-β^4 model, resolving one of the difficulties with X(5) by the presence of a softer outer potential (an automatic feature of the β^4 potential

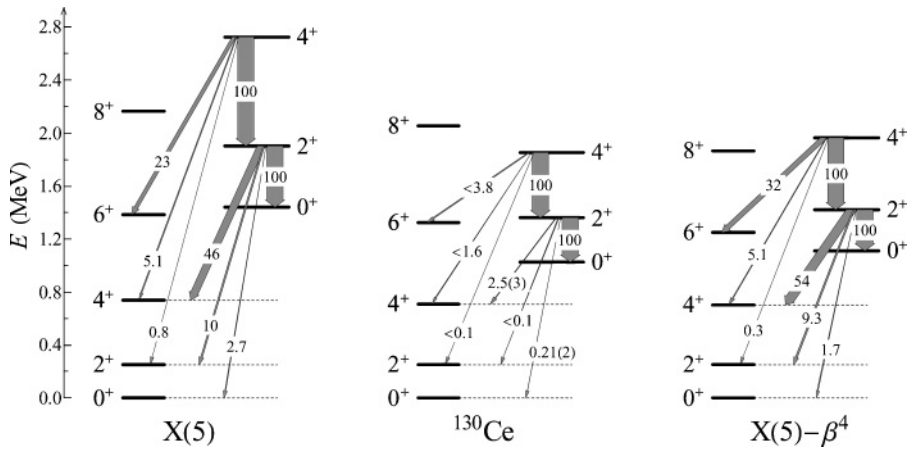

FIG. 7. Experimental level energies and relative $B(E2)$ strengths for ^{130}Ce compared with the predictions for the X(5) and X(5)-β^4 models. Energies are normalized to the experimental $E(2_1^+)$ value. $B(E2)$ values are normalized to the intraband transition with the strength indicated by the widths of the transition arrows.

and consistent with the results of Ref. [17] for an ad hoc sloped outer wall).

In terms of the relative branching ratios from the 2^+ and 4^+ members of the 0_2^+ band, the overall agreement is slightly worse (for the $J \rightarrow J+2$ transition) than the discrepancies with X(5) described above. As one moves to more vibrational nuclei, the 2^+ state of the 0_2^+ band can be considered as approaching a member of the $N = 3$ phonon multiplet. Thus, the transition to the 4_1^+ state, in particular, will become more collective. This disagrees strongly with the data on ^{130}Ce.

Both the X(5) and X(5)-β^4 models use an axially symmetric potential in the γ degree of freedom (harmonic oscillator with a minimum at $\gamma = 0^\circ$). However, the $A \sim 130$ Xe-Ba region has previously been described [19,20] as exhibiting a more γ soft structure. Although data such as $R_{4/2}$ or $E(2_\gamma^+)/E(2_1^+)$ suggest that for a given neutron number, the Ce isotopes are somewhat more deformed and more axially symmetric than the Ba or Xe isotopes, this nevertheless suggests that the discrepancies with the relative $B(E2)$ values might be related to the γ degree of freedom. To investigate this possibility, we applied a more flexible model which allows us to vary the softness of the potential in the γ degree of freedom.

To introduce the γ degree of freedom, we performed two-parameter interacting boson approximation (IBA-1) [21] calculations using the Hamiltonian [22]

$$H(\zeta, \chi) = a\left[(1-\zeta)\hat{n}_d - \frac{\zeta}{4N_B}\hat{Q}^\chi \cdot \hat{Q}^\chi\right], \qquad (2)$$

where $\hat{n}_d = d^\dagger \cdot \tilde{d}$, and $\hat{Q}^\chi = (s^\dagger \tilde{d} + d^\dagger s) + \chi(d^\dagger \tilde{d})^{(2)}$. Electromagnetic transitions are calculated using the $E2$ operator, $T(E2) = e_B Q$. Calculations were performed by diagonalizing the Hamiltonian numerically using the computer code PHINT [23]. The two free parameters are ζ and χ, and $N_B = 9$ is the number of valence bosons. The parameter χ controls the degree of γ softness: $\chi = -1.32$ gives an axially symmetric potential in γ, while $\chi = 0$ corresponds to a γ-flat potential. We obtain a reasonable description of ^{130}Ce with the parameters $\zeta = 0.77$ and $\chi = -0.30$.

A comparison between these IBA calculations and ^{130}Ce is given in Fig. 8. The IBA provides a reasonable description of the yrast band energies and the γ-band energies. The 0_2^+ energy is overpredicted in the IBA by about 300 keV, and the spacing in the 0_2^+ sequence is expanded in the IBA calculations relative to the data. This is again similar to what is observed in the X(5) predictions. Still, we do observe a strong overall reduction in the interband $B(E2)$ transition strengths between the excited 0^+ band and the ground-state band in the present IBA calculations compared with the geometrical models discussed above. Note that a χ value of -0.30 is intermediate between the SU(3) and O(6) limiting values. The $2^+_{K=0_2^+} \rightarrow 4_1^+$ transition strength is reduced by a factor of 5 in the IBA calculations compared with the X(5)-β^4 predictions, but still is slightly larger than observed in the data. The transition strengths to the 2_1^+ and 0_1^+ levels are now reasonably reproduced by the IBA calculations. In addition the decay from the 4_γ^+ level is consistent with the data.

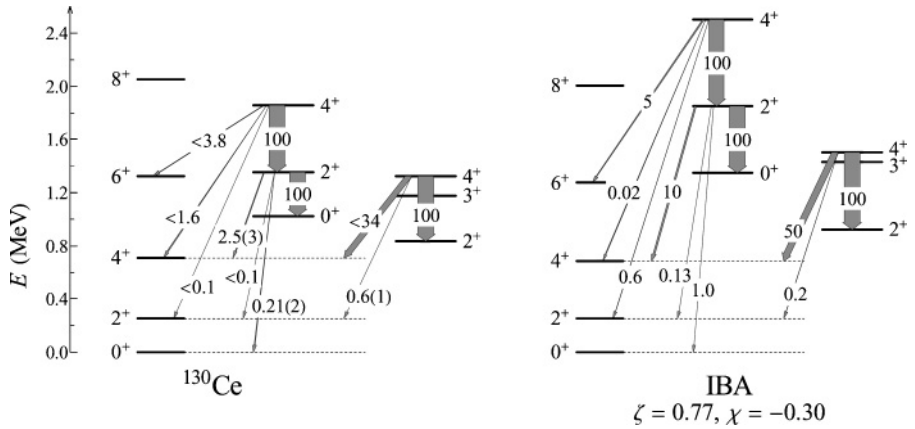

FIG. 8. Experimental level energies and relative $B(E2)$ strengths for ^{130}Ce compared with IBA calculations. Energies are normalized to the experimental $E(2_1^+)$ value. $B(E2)$ values are normalized to the intraband transition with the strengths indicated by the widths of the transition arrows.

IV. CONCLUSION

Off-beam γ-ray spectroscopy was performed on ^{130}Ce populated in β^+/ϵ decay. New coincidence data allowed for the revision of several low-lying levels important to the structural interpretation of ^{130}Ce. An initial comparison of ^{130}Ce to the predictions of the X(5) critical-point model points to ^{130}Ce lying slightly to the spherical-vibrator side of the phase transition. The X(5)-β^4 model, which describes the structure between a spherical vibrator and X(5), well describes the energies in ^{130}Ce but shows large discrepancies with the relative $B(E2)$ transition strengths. These disagreements perhaps can be attributed to ^{130}Ce having a potential in the γ degree of freedom which is softer than the axially symmetric potential assumed in the X(5) and X(5)-β^n models. This idea was tested by trying to describe ^{130}Ce using two-parameter IBA-1 calculations. The agreement, overall, is reasonable and the resulting χ value points to a structure that is intermediate between a γ-soft and axially symmetric potential in the γ degree of freedom. While the present work provides some evidence that the γ degree of freedom may need to be considered in this mass region, more extensive data are needed on the off-yrast structures of other potential X(5) candidates in this region.

ACKNOWLEDGEMENT

This work is supported by the U.S. DOE under Grant No. DE-FG02-91ER-40609.

[1] F. Iachello, Phys. Rev. Lett. **87**, 052502 (2001).
[2] F. Iachello, Phys. Rev. Lett. **85**, 3580 (2000).
[3] R. F. Casten and N. V. Zamfir, Phys. Rev. Lett. **87**, 052503 (2001).
[4] R. Krücken *et al*., Phys. Rev. Lett. **88**, 232501 (2002).
[5] D. Tonev *et al*., Phys. Rev. C **69**, 034334 (2004).
[6] R. F. Casten and E. A. McCutchan, J. Phys. G: Nucl. Part. Phys. **34**, R285 (2007).
[7] R. B. Cakirli and R. F. Casten, Phys. Rev. Lett. **96**, 132501 (2006).
[8] R. F. Casten, D. S. Brenner, and P. E. Haustein, Phys. Rev. Lett. **58**, 658 (1987).
[9] R. F. Casten, Phys. Rev. Lett. **54**, 1991 (1985).
[10] E. A. McCutchan, N. V. Zamfir, and R. F. Casten, J. Phys. G: Nucl. Part. Phys. **31**, S1485 (2005).
[11] B. Singh, Nucl. Data Sheets **93**, 33 (2001).
[12] R. M. Clark *et al*., Phys. Rev. C **68**, 037301 (2003).
[13] N. V. Zamfir and R. F. Casten, J. Res. Natl. Inst. Stand. Technol. **105**, 147 (2000).
[14] C. W. Beausang *et al*., Nucl. Instrum. Methods Phys. Res. A **452**, 431 (2000).
[15] A. Gizon, J. Genevey, C. F. Liang, P. Paris, D. Barnéoud, J. Inchaouh, I. Penev, and A. Plochocki, Eur. Phys. J. A **12**, 309 (2001).
[16] Yu. Khazov, I. Mitropolsky, and A. Rodionov, Nucl. Data Sheets **107**, 2715 (2006).
[17] M. A. Caprio, Phys. Rev. C **69**, 044307 (2004).
[18] D. Bonatsos, D. Lenis, N. Minkov, P. P. Raychev, and P. A. Terziev, Phys. Rev. C **69**, 014302 (2004).
[19] G. Puddu, O. Scholten, and T. Otsuka, Nucl. Phys. **A348**, 109 (1980).
[20] R. F. Casten and P. von Brentano, Phys. Lett. **B152**, 22 (1985).
[21] F. Iachello and A. Arima, *The Interacting Boson Model* (Cambridge University Press, Cambridge, 1987).
[22] V. Werner, N. Pietralla, P. von Brentano, R. F. Casten, and R. V. Jolos, Phys. Rev. C **61**, 021301(R) (2000).
[23] O. Scholten, KVI-63, Groningen (unpublished).